Available online at www.sciencedirect.com

ScienceDirect

Mendeleev Commun., 2016, **26**, 231–234

Mendeleev
Communications

One-pot preparation of SERS nanocomposites of silver and graphene oxide with tunable properties

Mariia O. Volodina,[a] Alexander Yu. Polyakov,[b] Alexander V. Sidorov,[b,c] Anastasia V. Grigorieva,[b] Elena A. Eremina,[a,b] Serguei V. Savilov[a] and Eugene A. Goodilin*[a,b,d]

[a] *Department of Chemistry, M. V. Lomonosov Moscow State University, 119991 Moscow, Russian Federation. Fax: +7 495 939 0998; e-mail: goodilin@yandex.ru, goodilin@inorg.chem.msu.ru*
[b] *Department of Materials Science, M. V. Lomonosov Moscow State University, 119991 Moscow, Russian Federation*
[c] *National Research Centre 'Kurchatov Institute', 123098 Moscow, Russian Federation*
[d] *N. S. Kurnakov Institute of General and Inorganic Chemistry, Russian Academy of Sciences, 119991 Moscow, Russian Federation*

DOI: 10.1016/j.mencom.2016.05.003

Surface-enhanced Raman spectroscopy-active nanocomposites of silver and graphene oxide were obtained by ultrasonic aerosol spray pyrolysis of graphene oxide suspension in diamminesilver(I) hydroxide aqueous solution thus allowing one to tune silver nanoparticle load, size and an overall specific area of the nanocomposite.

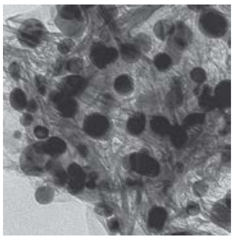

Graphene is currently the most intensively studied material for a wide range of applications including electronics, solar energy, batteries and sensors.[1–4] It is biocompatible and seems to have superior properties compared to other sensor materials.[3,5] In particular, graphene-based materials have unique chemical and physical properties which make them very promising for applications in biology and, particularly, for surface-enhanced Raman spectroscopy (SERS) in medical diagnostics.[2,3,6–11] Graphene oxide (GO) is a convenient construction block for building and self-assembling nanocomposites including GO–metal nanoparticles materials.[6–20] The GO precursor offers the unique advantage of tunable physical and chemical properties which can be achieved simply by oxidizing or reducing GO. This can drastically change the types and amounts of functional groups and defects associated with GO.[12,13] A usual way to create a GO–metal nanocomposite includes a separate synthesis of noble metal nanoparticles and their binding to the surface of GO using electrostatic forces or chemical interactions with thiols or amines.[6–11] Only in few works, nucleation and growth of plasmonic nanoparticles in the presence of GO is suggested by soft chemistry methods.[10,15–20]

Aerosol spray pyrolysis (ASP) is an effective streaming and scalable method based on spraying of micrometre-sized droplets of precursor solutions and their fast nonequilibrium transformation at high temperatures into solid phases and nanostructured materials.[11,21–23] The droplets play the role of microreactors often providing such nanostructuring.[21] Unfortunately, application of this technique with respect to GO and noble metal nanocomposites is limited at the moment and focused on gold nanoparticles mostly.[11] At the same time, GO itself can serve as either a reducing or anchoring agent specifically for silver ions; therefore, Ag@GO nanocomposites would benefit from these properties. In this work, the ASP method was applied for the first time to produce effectively and in one step Ag@GO nanostructures with tuned nanoparticle load, sizes and an overall specific area of the nanocomposite and also graphene oxide mediated SERS substrates. Both the routes for the nanoparticles and the substrates are basically same and include a new effective and scalable streaming procedure based on diamminesilver hydroxide self-reduction on the surface of GO flakes. $[Ag(NH_3)_2]^+$ derivatives are suitable precursors for the preparation of pure silver nanoparticles even without an application of additional reagents thus providing new possibilities for Ag-based biocompatible SERS material formation.[21,22]

The colloidal GO was prepared by the modified Hammers method of oxidation of graphite powder (TIMCAL TIMREX® KS4, 99.9%).[12] In brief, graphite powder was mixed with sodium nitrate and 98% sulfuric acid inside an ice bath and then $KMnO_4$ was slowly added under magnetic stirring at temperature lower than 70 °C. The obtained brownish mixture was accurately diluted with distilled water, then remained $KMnO_4$ and MnO_2 were reduced and dissolved using 3% H_2O_2, while the color of the mixture turned into yellow. The suspension of graphene oxide was left to stay overnight to complete all the reduction processes and then it was centrifuged and washed with distilled water for at least three times.

To prepare the Ag@GO nanocomposites, a precursor suspension of GO was mixed with 0.01 M $[Ag(NH_3)_2]OH$ aqueous solution in volumetric ratios of 1:1, 10:1 and 100:1, respectively, while the original concentration of GO was fixed at about 3.9×10^{-2} M. Diamminesilver solution was simply prepared by dissolution of silver nitrate in pure water, precipitation of silver(I) oxide with 0.5 M sodium hydroxide, washing and adding aqueous ammonia as described.[21,22]

After that, the precursor mixture was transformed into an aerosol stream by an ultrasonic nebulizer and decomposed in a hot zone of a tubular furnace (600–800 °C) followed by collecting the resulting powder onto a porous glass filter. To form the GO mediated SERS substrates, the 1:1 precursor mixture of colloidal

GO and $[Ag(NH_3)_2]OH$ solutions was nebulized and deposited for 20–30 min onto the surface of standard glass plates heated up to 280–300 °C in air.

The nanoparticle size distribution and morphologies of the obtained Ag@GO nanocomposites were investigated by a scanning (SEM, Zeiss NVision 40-38-50) and transmission electron microscopy (TEM, LEO 912 AB Omega). Raman and SERS experiments were performed using InVia Raman microscope (Renishaw, UK) equipped with a 20 mW 514 nm argon laser and power neutral density filter (10%). All the spectra were collected using 20× objective lens and 10 s of acquisition time. A silicon wafer was used for calibration. XPS analysis was performed with a Kratos AXIS Ultra DLD spectrometer. An Al Kα monochromated radiation ($h\nu$ = 1486.6 eV) was employed as an X-ray source. The values of specific surface areas were investigated by BET and BJH analysis (Quantachrome NOVA 4200e). Thermal analysis data were obtained by means of the Netsch autosampling system with a mass-spectrometry control of exhausting gaseous products.

As seen from Figure 1, the presence of GO and treatment temperatures are the most important preparation parameters of the Ag@GO nanocomposites (Table 1).

TEM images of pristine GO reveal that the size of prepared GO sheets in a colloidal mixture was about 1–15 μm. The Raman spectrum showed a G band at 1598 cm^{-1} and D band at 1351 cm^{-1}, with an intensity ratio I_D/I_G = 0.93 meaning that the obtained GO was extensively oxidized. The XPS spectrum contained peaks from various functional groups on the GO surface: O-contained (14.46% of C–O bond, 27.47% of C=O, 0.82% of COOR). C–C bond of *sp*^{2} carbon atoms contributed as 23.56%, with a molar ratio of C : O = 1.21 (Figure 2).

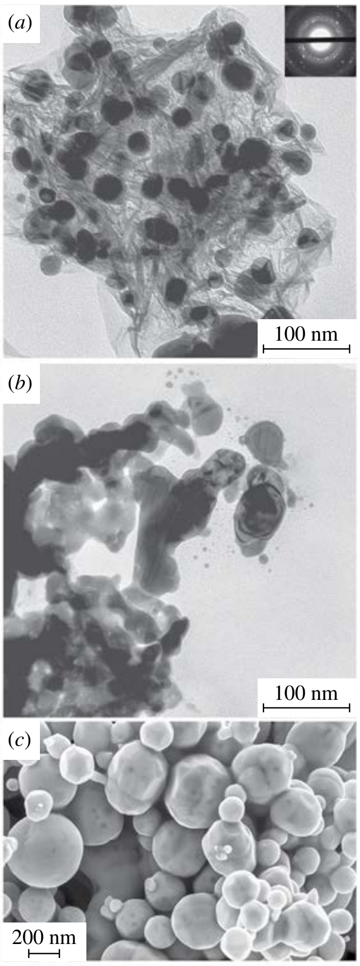

Figure 1 Microstructures of Ag@GO nanocomposites prepared by ultrasonic aerosol spray pyrolysis using diamminesilver solutions and GO suspensions. (*a*) Ag@GO prepared at 600 °C in a furnace hot zone, the ratio of GO and diamminesilver solution is 10:1, the inset shows SAED of silver nanoparticles; (*b*) an increase in the preparation temperature up to 800 °C; (*c*) ASP of pure 0.01 M $[Ag(NH_3)_2]OH$ at 600 °C.

Table 1 Ag@GO morphology.

Sample GO/AgNPs[a]		Size of AgNPs/nm
T/°C	*c*(GO) : *c*(Ag$^+$)	
600	1:1	40±25
	10:1	30±15
	100:1	5–80
800	1:1	5–300
	10:1	5–200
	100:1	15–50
300	1:1	50±20

[a] AgNPs – silver nanoparticles.

Almost the same GO flake size remains after ASP preparation of Ag@GO nanocomposite at 600 °C [Figure 1(*a*)]. Despite the presence of oxygen in carrier air, nanocomposites were preserved due to lowering a real temperature because of evaporation of water from droplets and creation of a reducing atmosphere because of a high concentration of ammonia in the precursor mixture. TEM images showed that the ASP synthesis afforded Ag@GO nanocomposites of different loadings of GO sheets with silver nanoparticles possessing simultaneously different sizes. By varying concentration of reagents under 600 °C of aerosol decomposition, the silver nanoparticles size of 30–40 nm was achieved for the 1:1 and 10:1 concentration ratios, respectively (Table 1), as optimal for SERS. Those conditions allowed us to reach different values of specific surface areas of the nanocomposites, namely, 10 m^2 g^{-1} for the sample with a precursor mixture ratio of 1:1 and a much higher area of 99 m^2 g^{-1} for the ratio 10:1. A small amount of silver for the ratio of 100:1 leads to very nonuniform coating of GO flakes with AgNPs and a wide deviation in particle sizes, thus this ratio is excluded from further considerations. Higher preparation temperatures of about 800 °C were unfavourable causing fast nanoparticle coarsening, agglomeration (Table 1) and partial thermal damage of GO flakes [Figure 1(*b*)]. Decomposition of pure diamminesilver aqueous aerosol [Figure 1(*c*)] leads to large facetted spherical particles of silver with a high deviation amplitude of their sizes; most of them might not have effective SERS properties. Thus, rather low preparation temperatures (600 °C), an average amount of silver ions (10:1) and the presence of GO are necessary to produce promising Ag@GO nanocomposites with a high silver load, appropriate silver nanoparticle sizes and a high (about 100 m^2 g^{-1}) specific surface area.

The obvious effect of GO on silver nanoparticle nucleation and growth is directly linked to the chemistry of its functional groups (Figure 2). Pure GO demonstrates two exothermic effects associated with weight loss and CO_2 liberation, at *ca*. 100–150 °C and 500–550 °C [Figure 2(*h*)]. The first of them manifests so-called 'reduction' of GO with the formation of reduced GO (r-GO), which means that the *sp*^{2} carbon network is recovered partly due to the loss of most of functional groups linked to *sp*^{3} carbons followed by their oxidation in air into CO_2. However, in the case of diamminesilver, this event generates most probably multiple silver nuclei attached directly to the surface of GO. This results, in turn, in a smaller average size of final ASP-prepared silver nanoparticless of the Ag@GO nanocomposites as compared to decomposition of pure $Ag[(NH_3)_2]OH$ (Figure 1). The second event above 550 °C comes from carbon burning, however, it starts at higher temperatures and is prevented by water vapor and ammonia present in the course of the synthesis.

XPS data confirm our hypotheses. First of all, Ag@GO nanocomposite formation preserves carbon networks and increases

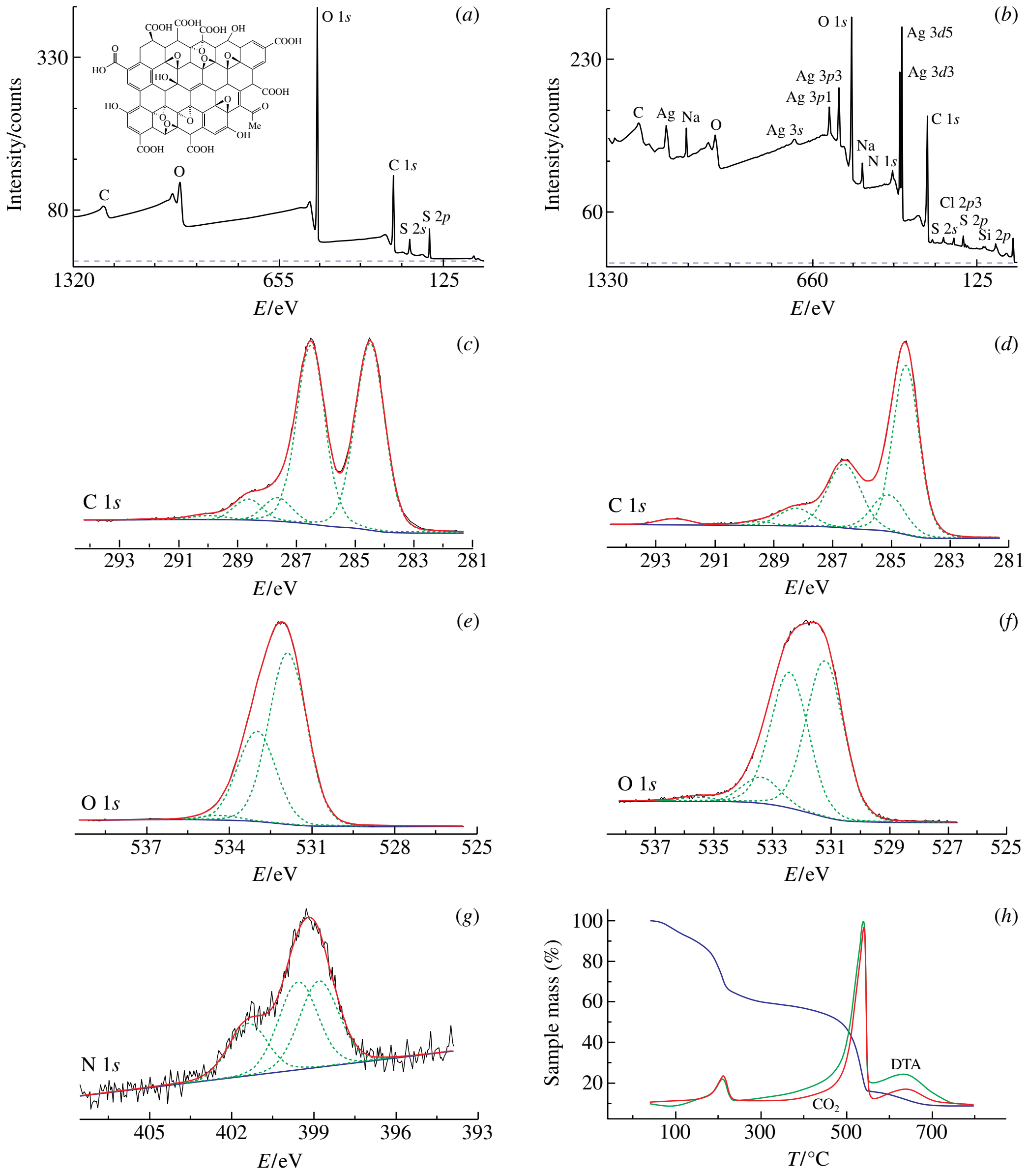

Figure 2 Chemical analysis data of an as-prepared GO precursor and Ag@GO nanocomposites, in comparison. Survey XPS spectra of (*a*) GO (the inset shows schematically typical functional groups of GO) and (*b*) Ag@GO prepared at 600 °C; C 1*s* XPS peak analysis for (*c*) GO and (*d*) Ag@GO, note an observed decrease in the ratio of O 1*s* to C 1*s* peaks and the appearance of intense silver lines; O 1*s* XPS peak analysis for (*e*) GO and (*f*) Ag@GO; (*g*) N 1*s* XPS peak analysis for Ag@GO, the same data for pure GO are negligibly low intense; (*h*) thermal analysis data for pure GO, DTA exothermal events, the CO_2 notation means the carbon dioxide presence in the outlet gaseous phase.

C 1*s* components overall contribution by 8% (from 51.7% for pure GO up to 59.7%) (Figure 2). This is even a larger increase in carbon content since ASP with diamminesilver adds 5.1% of silver atoms and also 2.6% of nitrogen which is a half of pyridine-like fragments and also would be a part of CH_2NR_2, RCN, CONH or, to a smaller extent, NR_4^+ groups. The N 1*s* peak appears for Ag@GO [Figure 2(*g*)].

This seems to be beneficial because such doping strengthens an attachment of silver nanoparticles to GO sheets since silver has normally good coordination constants with nitrogen ligands. At the same time, the oxygen O 1*s* component contribution decreases from 42.8% down to 26.6%, which means GO reduction as described above. The sp^2 ‘nanocarbon’ component at 284.5 eV rises up from 23.6 to 30.3%, while the C–O-like carbon at 286.6 eV falls down from 21.8 to 14.6%, for the Ag@GO samples [Figure 2(*c*),(*d*)] that would mean consumption of epoxy and alkoxy groups for silver ion reduction followed by silver nanoparticle nucleation on the original GO. The same is confirmed by the oxygen C=O component reduction at 531.2 eV from 27.5% down to 12.9% and the C–O component decrease at 533.4 eV from 14.5 to 2.5%. The carboxyl oxygen content at 532.4 eV rises from 0.8 to 11.2%, as expected. Finally the molar ratio of C:O becomes 2.25. A small enough amount of oxygen would indirectly confirm the formation of metallic silver instead of Ag_2O as also evident from SAED (Figure 1).

Immobilization of SERS-active nanomaterials in order to prepare substrates for optical analysis is known to be an effective way to expand and advance practical applications of SERS.[21] Ag@GO nanocomposites possess properties which make them especially suitable for creating multifunctional materials. These properties include variable hydrophobicity,[2] an increased specific surface area, hypothetically, the affinity to analytes complementary to superficial groups provided by artificial chemical modification. Therefore, in this work, we applied the same ASP procedure to deposit Ag@GO onto a surface of glassy substrates rather than to heat aerosol and collect its reaction products on a porous glass filters. This modification changes almost nothing from a chemical point of view but results in a suitable material for a possible SERS analysis. To achieve a uniform coverage of the substrate surface, the substrates were preheated up to 300 °C to allow chemical decomposition of the precursor suspension to occur and to form Ag@GO nanocomposites on the substrates directly (Figure 3). ASP deposition of the precursor suspension gives intersecting circles of 40–60 μm in diameter [Figure 3(*a*)]. This value is several times larger than the expected size of falling mist droplets and therefore the liquid from the droplets, indeed, spreads laterally over the substrate. Solvent evaporation increases concentration of the silver complex and then metallic silver resides on rims of the spreading circles producing walls of GO craters decorated with metallic silver nanoparticles. The size of silver nanoparticles was found to be about 50 nm [Figure 3(*b*)]. Most of the circles form groups or long chains until the surface becomes rather uniformly covered with stochastically intersecting silver rings.[21] Such a rough microstructure allows one to distribute analyte droplets over the surface and perform a SERS analysis. In particular, the substrates register a signal from a model dye of Rodamine 6G [Figure 3(*c*)].

In conclusion, a new one-pot synthesis of SERS-active nanocomposites of silver and graphene oxide is developed for the first time using of a versatile and effective method of ultrasonic aerosol spray pyrolysis of GO suspension in diamminesilver aqueous solution thus making it possible to tune over silver nanoparticle loading, sizes and overall specific area of the nanocomposite. The basis of the whole process is reduction of silver ions with GO functional groups to nucleate and grow silver nanoparticles demonstrating SERS-activity in a form of such a nanocomposite. Further works in this direction are in progress to find its scope and limitations and to search for other practical applications of such nanocomposites.[7–14,24]

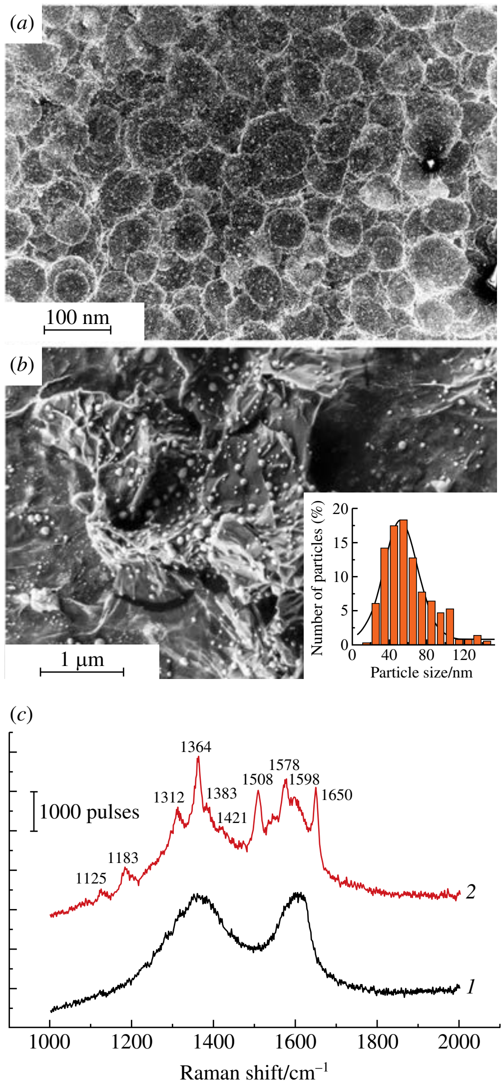

Figure 3 SERS data obtained using substrates with AG@GO layers sputtered by ASP at 280–300 °C for 20–30 min. (*a*) An overall microstructure demonstrating a circular morphology appearing due to aerosol droplet spreading and evaporation on the preheated surface, (*b*) spherical nanoparticles of silver and their size distribution (shown in the inset), (*c*) SERS spectra of the Rhodamine 6G dye with (*1*) 10^{-8} and (*2*) 10^{-6} mol dm^{-3} concentrations.

This work was supported by the Russian Science Foundation (grant no. 14-13-00871). The authors acknowledge partial support from M. V. Lomonosov Moscow State University Program of Development for providing analytical research of the materials.

References

1 K. S. Novoselov, A. K. Geim, S. V. Morozov, D. Jiang, Y. Zhang, S. V. Dubonos, I. V. Grigorieva and A. A. Firsov, *Science*, 2004, **306**, 666.
2 P. T. Yin, S. Shah, M. Chhowalla and K.-B. Lee, *Chem. Rev*., 2015, **115**, 2483.
3 Yu. D. Tretyakov and E. A. Goodilin, *Russ. Chem. Rev*., 2009, **78**, 801 (*Usp. Khim*., 2009, **78**, 867).
4 D. A. Semenenko, D. M. Itkis, E. A. Pomerantseva, E. A. Goodilin, T. L. Kulova, A. M. Skundin and Yu. D. Tretyakov, *Electrochem. Commun*., 2010, **12**, 1154.
5 A. V. Grigorieva, A. B. Tarasov, E. A. Goodilin, S. M. Badalyan, M. N. Rumyantseva, A. M. Gaskov, A. Birkner and Yu. D. Tretyakov, *Mendeleev Commun*., 2008, **18**, 6.
6 S. Jiao, Y. Wang, C. Chen, X. Wu and F. Bei, *J. Mol. Struct*., 2014, **1062**, 48.
7 W. Ren, Y. Fang and E. Wang, *ACS Nano*, 2011, **5**, 6425.
8 V. K. Gupta, N. Atar, M. L. Yola, M. Eryılmaz, H. Torul, U. Tamer, İ. H. Boyacı and Z. Üstündağ, *J. Colloid Interface Sci*., 2013, **406**, 231.
9 X. Liu, L. Cao, W. Song, K. Aia nd L. Lu, *ACS Appl. Mater. Interfaces*, 2011, **3**, 2944.
10 H. Hou, P. Wang, J. Zhang, C. Li and Y. Jin, *ACS Appl. Mater. Interfaces*, 2015, **7**, 18038.
11 H. D. Jang, S. K. Kim, H. Chang and J.-W. Choi, *Biosens. Bioelectron.*, 2015, **63**, 546.
12 W. S. Hummers and R. E. Offeman, *J. Am. Chem. Soc*., 1958, **80**, 1339.
13 D. C. Marcano, D. V. Kosynkin, J. M. Berlin, A. Sinitskii, A. Slesarev, L. B. Alemany, W. Lu and J. M. Tour, *ACS Nano*, 2010, **4**, 4806.
14 L. Li, B. An, A. Lahiri, P. Wang and Y. Fang, *Carbon*, 2013, **65**, 359.
15 G. Goncalves, P. A. A. P. Marques, C. M. Granadeiro, H. I. S. Nogueira, M. K. Singh and J. Grácio, *Chem. Mater*., 2009, **21**, 4796.
16 G. H. Ding, S. Xie, Y. Liu, L. Wang and F. G. Xu, *Appl. Surface Sci*., 2015, **345**, 310.
17 T. Gong, Y. Zhu, J. Zhang, W. Ren, J. Quan and N. Wang, *Carbon*, 2015, **87**, 385.
18 Y. Zhao and Y. Zhu, *Nanoscale*, 2015, **7**, 14561.
19 Y. Li, X. Zhao, P. Zhang, P. J. Ning, J. Li, Z. Su and G. Wei, *J. Mater. Chem. C*, 2015, **3**, 4126.
20 S. Murphy, L. Huang and P. V. Kamat, *J. Phys. Chem. C*, 2013, **117**, 4740.
21 A. A. Semenova, E. A. Goodilin, N. A. Brazhe, V. K. Ivanov, A. E. Baranchikov, V. A. Lebedev, A. E. Goldt, O. V. Sosnovtseva, S. V. Savilov, A. V. Egorov, A. R. Brazhe, E. Y. Parshina, O. G. Luneva, G. V. Maksimov and Yu. D. Tretyakov, *J. Mater. Chem*., 2012, **22**, 24530.
22 A. A. Semenova, N. A. Brazhe, E. Yu. Parshina, V. K. Ivanov, G. V. Maksimov and E. A. Goodilin, *Plasmonics*, 2014, **9**, 227.
23 H. D. Jang, S. K. Kim, H. Chang, E. H. Jo, K. M. Roh, J.-H. Choi and J.-W. Choi, *Aerosol Sci. Technol*., 2015, **49**, 538.
24 E. O. Pentsak and V. P. Ananikov, *Mendeleev Commun*., 2014, **24**, 327.

Received: 21st August 2015; Com. 15/4710